

SUPPLEMENTARY INFORMATION

Antimicrobial Hydrogels Incorporating Nanoselenium@Reduced Graphene Oxide Nanocomposites for Biofilm Inhibition

Deepa Garg^{a,b}, Vijayesh Kumar^{a,b}, Mercy Merlin S S^{a,b},

Abhay Sachdev^{a,b}, Ishita Matai^{c*}*

*^a Materials Science & Sensor Application Division, CSIR-Central Scientific
Instruments Organization (CSIR-CSIO), Chandigarh-160030, India.*

*^b Academy of Scientific and Innovative Research, Ghaziabad-201002, Uttar
Pradesh, India.*

^cDepartment of Biotechnology, Amity University Punjab, Mohali 140306, India

* Corresponding authors: AS: abhay.sachdev@csio.res.in;

IM: imatai@pb.amity.edu

Experimental Section

Materials. All the chemicals were of reagent grade, and used without any purification. Fresh Indian gooseberry (*Phyllanthus emblica*) fruit was purchased from the local market. Sodium selenite (Na_2SeO_3 , purity 99 %), and lysozyme were procured from Sigma-Aldrich, India. Gum Tragacanth (GT) was obtained from Loba Chemicals. Ammonium persulfate (APS), N,N'-Methylenebisacrylamide (MBAA), Tetramethylethylenediamine (TEMED), Acrylamide (AAM), Phosphate Buffer Saline (PBS), Phosphate Buffer (PB), Nutrient Broth (NB), Nutrient Agar (NA), Luria Broth (LB), and Tryptic Soy Broth (TSB) were purchased from Himedia, India. An antibiotic gentamicin was purchased from the local chemist. All the preparations were made using deionized (DI) water. Standard bacterial strains of *Pseudomonas aeruginosa* (MTCC 1688) and *Staphylococcus aureus* (MTCC 737) were obtained from Microbial Type Culture Collection Centre (MTCC), Institute of Microbial Technology, Chandigarh, India.

Characterization of the nSe@rGO nanocomposite

The absorption spectra of the samples were recorded using a UV-visible spectrophotometer (Cary 4000, India) in the wavelength range of 200-800 nm at 25°C. The X-ray Diffraction (XRD) pattern was obtained using a Model D8 Advance X-ray diffractometer (manufactured by Bruker AXS, Germany) at 25°C. Monochromatic Cu-K α radiation ($\lambda = 1.5406 \text{ \AA}$) was utilized in the angular range of 5-80°, with a scan rate of 1° per minute. Raman spectra of the samples prepared at 25°C were collected using a Raman analyzer (Renishaw, UK) equipped with a helium-neon laser with an excitation wavelength of 514 nm. The size and morphological features of the samples were assessed using a High Resolution-Transmission Electron Microscope (HR-TEM, JEOL JEM 2100 plus), equipped with Energy-Dispersive X-ray (EDX) Spectroscopy. TEM analysis involved drop-casting ~30 μL of the sample onto a carbon-coated copper grid, followed by thorough air drying at 25°C before analysis. The charge distribution was conducted by measuring the zeta potential (ζ) using a Malvern Zetasizer (ZS90) (Worcestershire, UK) at 25°C. For analysis, 50 μL of the samples were dispersed in DI water using a bath sonicator for 15 min at 30°C. The X-ray photoelectron spectroscopy (XPS) profiles were obtained using an X-ray Photoelectron Spectroscopy (PHI 5000 VersaProbe III). The chemical structure of the synthesized samples was analyzed by capturing Fourier Transform Infrared (FTIR) spectra using a Nicolet iS10 FTIR spectrophotometer within the range of 400 to 4000 cm^{-1} .

Characterization of nSe@rGO hydrogel

Morphological characterization. The morphology of the hydrogels was recorded by Field Emission Scanning Electron Microscopy (FESEM), at an accelerating voltage of 20 kV. The hydrogels of dimensions 10 x 10 mm² were swollen in DI water for 5-6 h at 37 °C, and freeze-dried using a lyophilizer operated at -56 °C. For better observation, the samples stored at RT were then coated with a thin layer of gold using a sputter coater, and images were recorded using FESEM.

Swelling behavior. The hydrogels prepared after gelation were cut in dimensions 10 x 10 mm² and weighed. They were then immersed separately in two different buffer solutions: PBS at pH 7.4 and PB at pH 5.5, both at 37 °C. At predetermined time intervals (1, 3, 5, 7, 12, 24, 48, and 72 h), the hydrogels were removed from the solutions, excess water was blotted using filter paper, and the weight of the swollen hydrogels was recorded. The percent swelling capacity was calculated using the following equation (1):

$$\% \text{ Swelling} = \frac{W_t - W_o}{W_o} \times 100, \quad (1)$$

wherein, W_t and W_o represent the weight of the swollen hydrogel at different times and the initial weight of the hydrogels before swelling, respectively.

Fourier Transform Infrared (FTIR) Spectroscopy. To analyze the chemical structure of the synthesized samples, FTIR spectra were recorded using a Nicolet iS10 FTIR spectrophotometer. The spectra were obtained in the range of 400 to 4000 cm⁻¹. Standard potassium bromide (KBr) pellets were used as the medium for sample preparation.

Release of nSe@rGO nanocomposite from the hydrogel. *In vitro* release from the 150 mg of hydrogel (nSe@rGO loading: ~200 µg) was performed in two different buffers: PBS (pH 7.4) and PB (pH 5.5)¹. The hydrogels were immersed into 5 mL of buffer in a glass vial and incubated at 37° C at 100 rpm. At predetermined intervals (1, 3, 6, 12, 24, 48, and 72 h), the vials with the buffer were taken out and 500 µL of the buffer was collected and subsequently replaced with an equal volume. To quantify the released nanocomposite, the absorption spectra of the aliquot samples were measured at 267 nm using UV-visible spectrometer. The concentration of the released

nanocomposite was determined by referencing calibration curves. The cumulative release (CR) was calculated based on the measured concentrations at specified time intervals.

Rheological behavior. The mechanical characteristics of the hydrogels were assessed using a rotational rheometer (Bohlin Rheometer CVO 100, Malvern Instruments Ltd.) equipped with 20 mm diameter parallel plate geometry. The disc-shaped hydrogels with a diameter of 22 mm and thickness of 1.5 mm were positioned on the lower plate at 25°C and the gap width was fixed at 1450 µm. To explore the linear viscoelastic region (LVR), strain-sweep tests were carried out at a strain amplitude varying from 0.1 to 500 % while maintaining a fixed angular frequency (ω) of 6.28 rad s⁻¹. Storage or elastic (G') and loss moduli (G'') were then measured using a frequency sweep test performed with an ω in the range of 0.6 - 439 rad s⁻¹, at a fixed strain calculated from the strain-sweep test.

In vitro enzymatic degradation. From the *in vitro* enzyme degradation assay, the stability of hydrogel network and degradation behavior were evaluated. Lysozyme was utilized as the primary model enzyme, following the methodology described by our previous publication ². Initially, pre-weighed hydrogels of dimensions 10 x 10 mm² were immersed in PBS with a pH of 7.4 for 12 h at 37°C to achieve equilibrium swelling. Subsequently, the swollen hydrogels were again soaked in a lysozyme solution (2 mg mL⁻¹, 3 mL) prepared in PBS buffer and incubated at 37°C. At specific time intervals (1, 3, 5, 7, 14, 21, and 28 days), the samples were removed, washed with deionized (DI) water, dried using Kimwipes, and weighed. Additionally, the lysozyme solution was replaced every three days to ensure consistent conditions. The extent of *in vitro* degradation of the hydrogels was assessed by calculating the percentage of residual mass using the following equation (2):

$$\% \text{ Residual mass} = \frac{W_t}{W_o} \times 100 \quad (2)$$

Here, W_o represents the weight of the hydrogel before immersion in lysozyme, and W_t represents the weight at different time intervals during the degradation assay.

Protein adsorption. To evaluate the antifouling capability of the hydrogels, their ability to resist protein adsorption was studied using the previously reported method with some modifications ³.

Briefly, the hydrogel samples of 10 x 10 mm² were soaked in a solution of 1.54 μM of BSA solution (10 mL, 1 mg mL⁻¹) prepared in PBS (pH 7.4) for 24 h at 37°C. After incubation, the hydrogels were removed from the soaking solution and washed thoroughly with 2 mL of PBS to remove loosely attached BSA protein. This washing solution was combined with the BSA soaking solution. Subsequently, the absorbance of the BSA solutions withdrawn was analyzed with a UV-Vis spectrophotometer at 280 nm. The relative adsorption of the BSA was calculated with respect to the initial concentration of the protein before hydrogel treatment, using the following equation (3):

$$(\%) \text{ Relative BSA Adsorption} = \frac{W_t}{W_o} \times 100 \quad (1-C_0/C_t) \times 100 \quad (3)$$

Here, C₀ and C_t represent the concentration of BSA before and after hydrogel treatment.

References

- 1 I. Matai, G. Kaur, S. Soni, A. Sachdev, Vikas and S. Mishra, *J Photochem Photobiol B*, 2020, **210**, 111960.
- 2 D. Garg, I. Matai, S. Agrawal and A. Sachdev, *Biofouling*, 2022, **38**, 965–983.
- 3 S. L. Banerjee, S. Samanta, S. Sarkar and N. K. Singha, *J Mater Chem B*, 2020, **8**, 226–243.

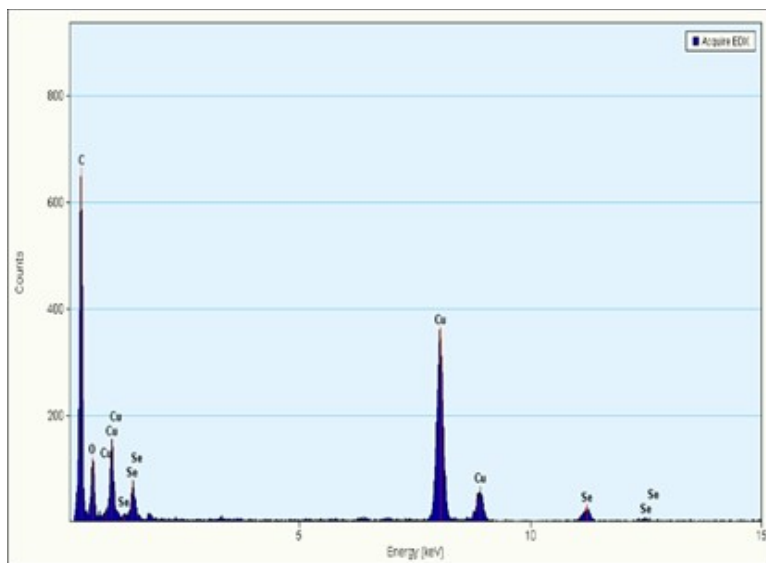


Figure S1. TEM-EDX spectrum of nSe@rGO nanocomposite.

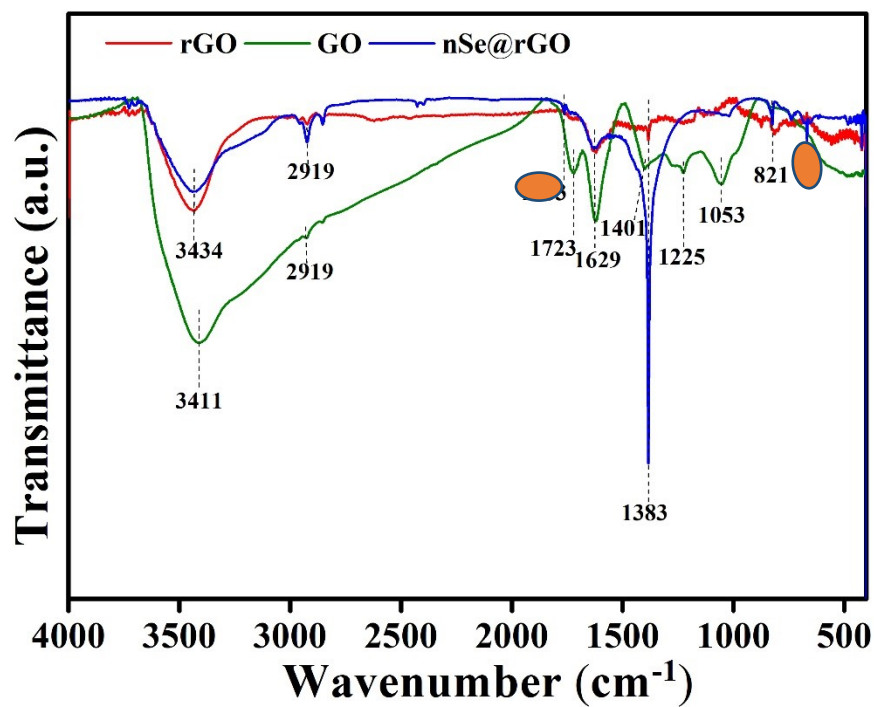


Figure S2. FTIR spectra of GO, rGO and nSe@rGO nanocomposite.

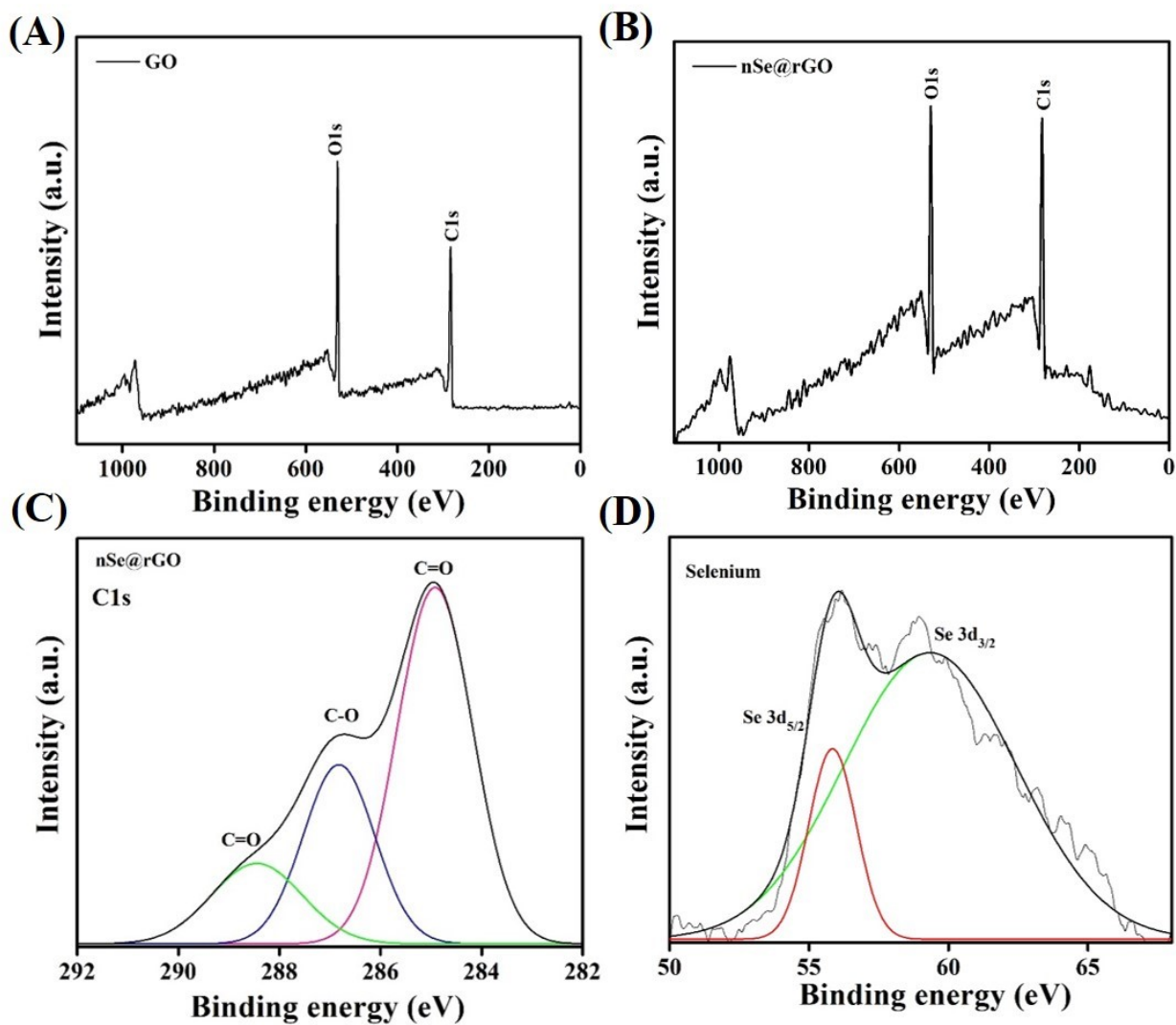


Figure S3. XPS Analysis. Wide spectra of (A) GO and (B) nSe@rGO nanocomposite. (C) Deconvoluted high-resolution C1s core spectra of nSe@rGO, (D) Deconvoluted high-resolution spectra of Se 3d of nSe@rGO.

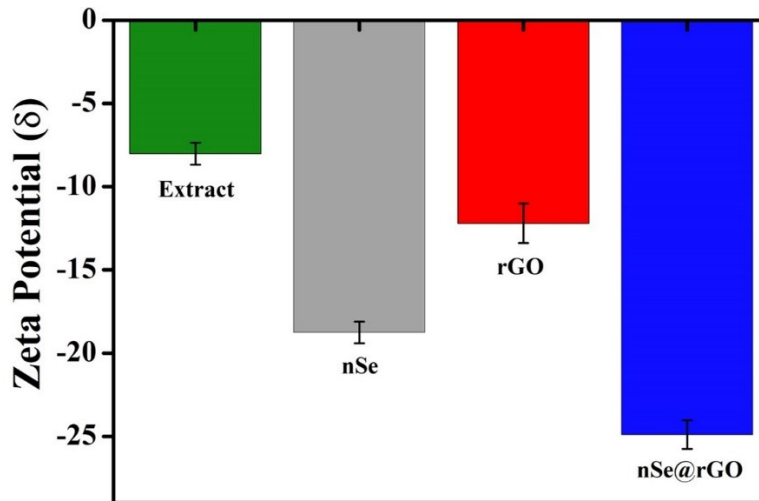
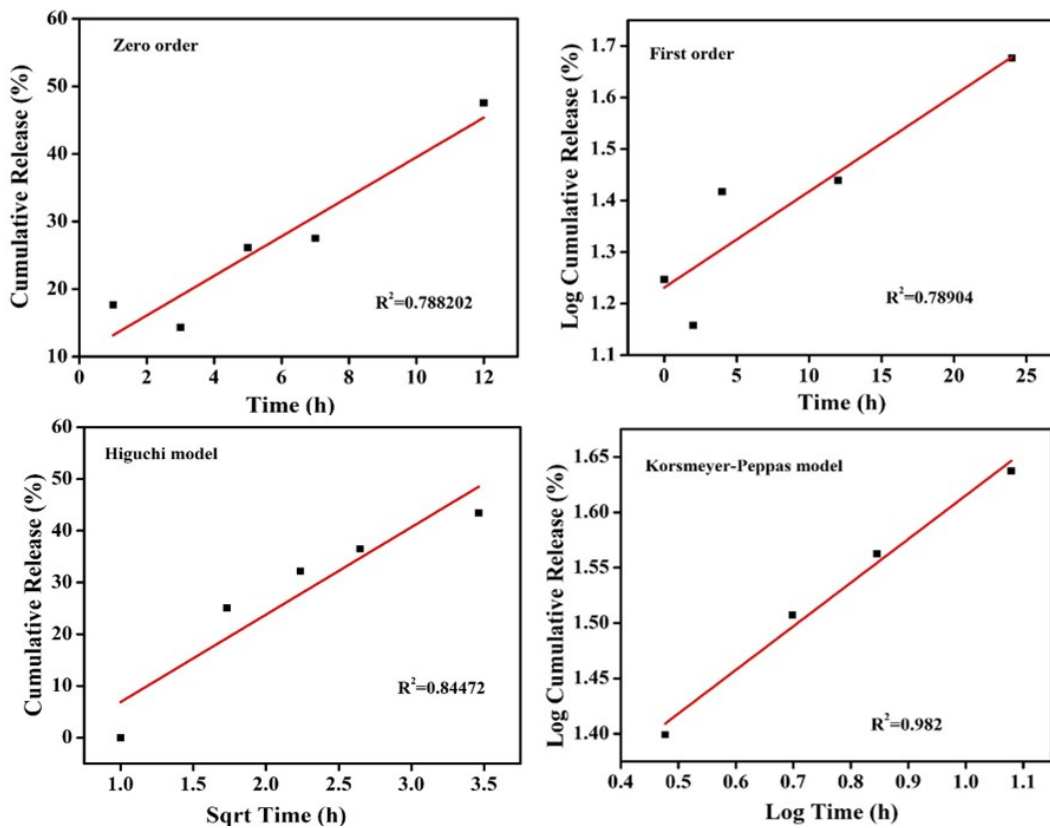


Figure S4. Zeta potential measurements of nSe, rGO and nSe@rGO nanocomposite.



Model	Formulation	Coefficient K	R ²
Zero-order	$Q_t = Q_0 + K_0 t$	2.29251	0.788326
First-order	$\ln Q_t = \ln Q_0 + K_1 t$	0.01865	0.78904
Higuchi	$Q_t = K_H t^{1/2}$	19.9056	0.84472
Korsmeyer-Peppas	$M_t/M_\infty = K t^n$	16.64, n = 0.3995 (Fickian diffusion)	0.98204

Figure S5. Different kinetic models and linear fitting for the release of nSe@rGO nanocomposite from the hydrogel at 37 °C.

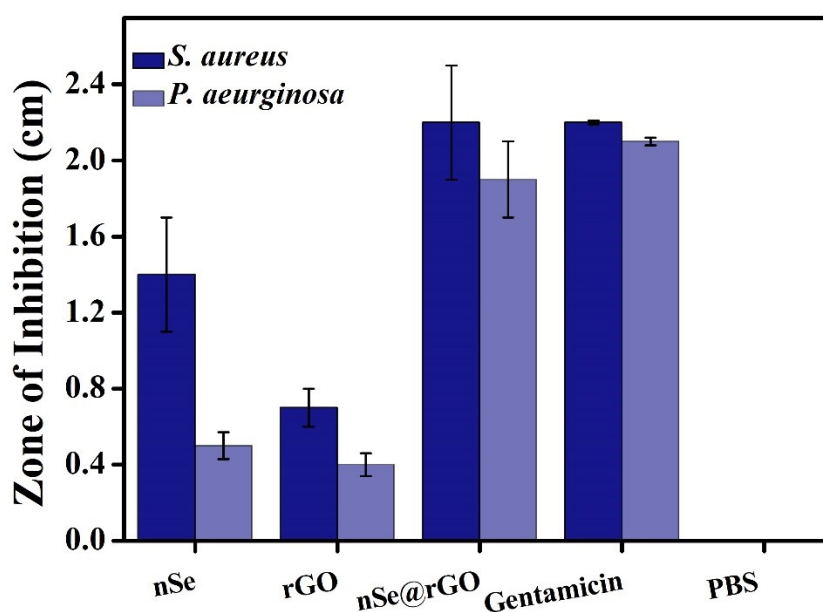


Figure S6. Zone of inhibition test of antibacterial materials against *S. aureus* and *P. aeruginosa* using agar well diffusion assay.

Bacteria	MIC ($\mu\text{g mL}^{-1}$)	MBC ($\mu\text{g mL}^{-1}$)
<i>S. aureus</i>	15	40
<i>P. aeruginosa</i>	20	62.5

Table S1. MIC and MBC for nSe@rGO nanocomposite.

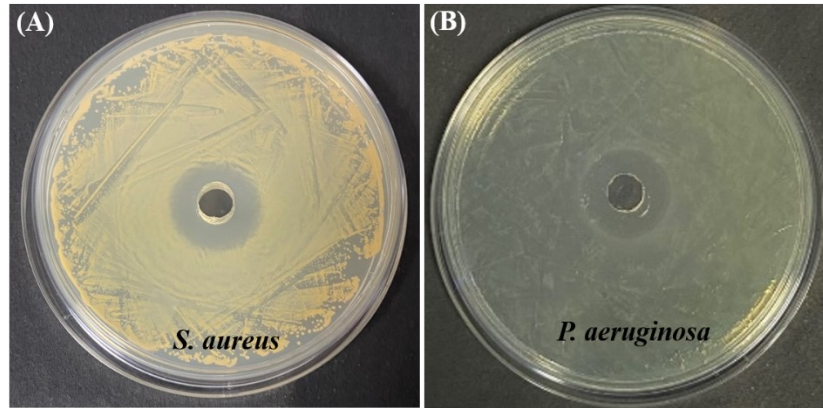


Figure S7. Agar well diffusion assay to estimate the ZOI of nSe@rGO hydrogel.

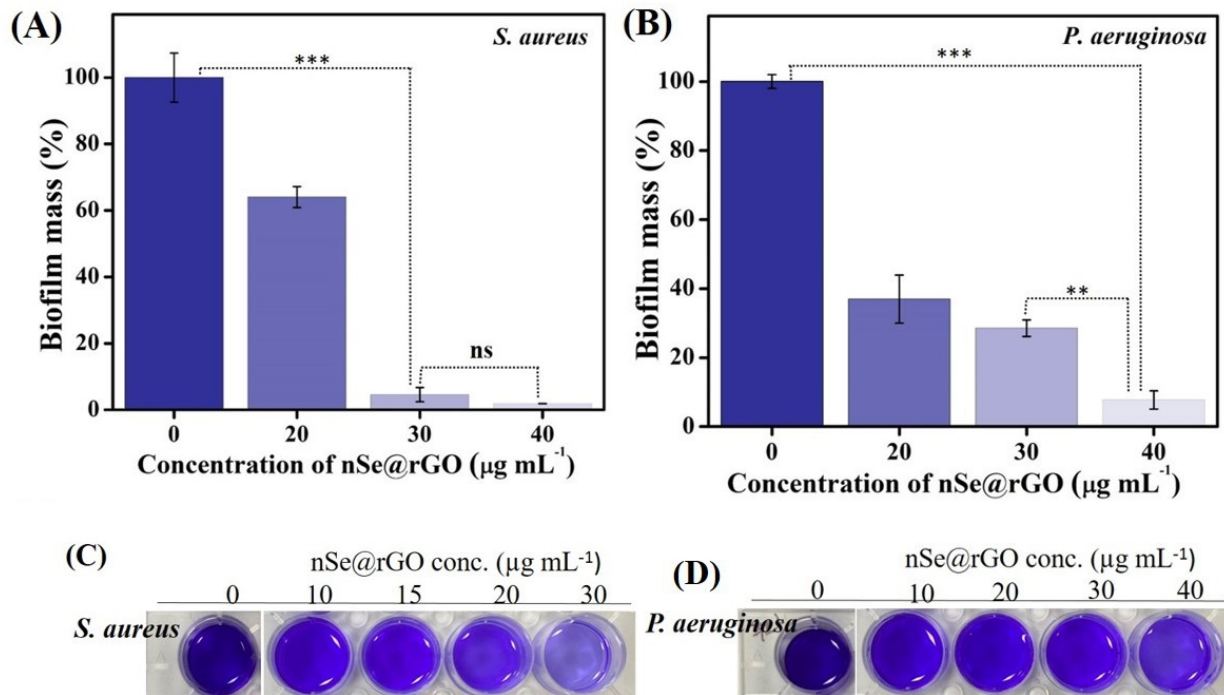


Figure S8. Determination of biofilm mass after treatment with nSe@rGO, as assessed by Crystal violet assay. Concentration-dependent biofilm inhibition of (A) *S. aureus*, and (B) *P. aeruginosa* after exposure to nSe@rGO for 24 h, and (C, D) representative digital images. The experiments were conducted in triplicate. Statistical analysis involved a one-way ANOVA followed by Tukey's multiple comparisons test to ascertain significant differences between the group means ($*p < 0.05$, $**p < 0.005$, $***p < 0.001$); ns denotes non-significant results.